ELSEVIER

Chemical Engineering Journal 138 (2008) 367–378

Chemical Engineering Journal

www.elsevier.com/locate/cej

Optimization of experimental procedure and statistical data treatment for kinetics of ethylene hydrogenation on a copper-magnesia catalyst

Sophie L. Pirard [a,*], Benoît Heinrichs [a], Georges Heyen [b], Jean-Paul Pirard [a]

[a] *Laboratoire de Génie Chimique, B6a, Université de Liège, B-4000 Liège, Belgium*

[b] *Laboratoire d'Analyse et de Synthèse des Systèmes Chimiques, B6a, Université de Liège, B-4000 Liège, Belgium*

Received 22 February 2007; received in revised form 31 May 2007; accepted 6 June 2007

Abstract

This study is an example of practical application of kinetic data treatment for simultaneous model discrimination and parameter estimation. The study is applied to the hydrogenation of ethylene on a copper-magnesia catalyst and brings a deepened analysis about the experimental strategy by comparing several alternative strategies using *a priori* and sequential experimental designs. The best model corresponds to a Langmuir–Hinshelwood mechanism with non-competing adsorption of hydrogen and ethylene and where the rate-determining step is either the addition of molecularly adsorbed hydrogen or the addition of the second atom of hydrogen adsorbed dissociatively. Furthermore, the important question of knowing in practice how many designs and how many measurements per design are actually necessary to determine accurate kinetic and physico-chemical parameters, is addressed. A data correction procedure is also presented that takes catalyst deactivation into account.
© 2007 Elsevier B.V. All rights reserved.

Keywords: Ethylene hydrogenation; Copper catalyst; Kinetics; Experimental design

1. Introduction

The hydrogenation of ethylene, the simplest olefin, has been investigated by many researchers as one of typical catalytic reactions since the classical work of Horiuti and Polanyi and the step-by-step reaction mechanism proposed by them in the 1930s [1]. Ethylene hydrogenation on a variety of catalytic surfaces has been extensively studied over years [2–7]. Numerous efforts have been devoted to the study of ethylene hydrogenation on well-defined crystallographic planes of transition metal catalysts (group VIII): Ru(0 0 1) [8], Pd(1 1 1) [9], Pt(1 1 1) [10], Rh(1 0 0) [11,12], Pd(1 1 0) [13], Ni(1 0 0) [14,15], and Cu [16,17]. Those studies essentially deal with the influence of surface coverage (preadsorption of ethylene [15,18], variation of partial pressures, surface coverage with a thin metallic film [12]) in order to better understand energetic bonds between species and the catalytic surface. Most often, authors suggest a reaction mechanism based on molecular adsorption of ethylene, dissociative adsorption of hydrogen, and the stepwise addition of hydrogen atoms to ethylene on the surface of the catalyst [1,19–21]. C_2H_4 and H_2 adsorb either competitively [1,19,20,22] or non-competitively [1,20,22,23]. On metals from group VIII, the apparent activation energy of ethylene hydrogenation most of the time lies in the range from 30 to 45 kJ mol^{-1} [20,21]. In the particular case of copper, activation energies between 17 and 82 kJ mol^{-1} have been found [21].

The present study deals with ethylene hydrogenation on a copper-magnesia catalyst. It is partly based on experimental data published previously [16] and it aims at proposing efficient statistical methodologies, based on *a priori* and/or sequential experimental designs, allowing to quickly identify the kinetic model that best fits the data and to estimate its parameters as precisely as possible with a small number of experiments. The necessary correction of experimental rate values to relate them to a reference activity level and its statistical implications are also addressed.

2. Experimental

2.1. Catalyst preparation

The catalyst used for this kinetic study was a Cu-MgO catalyst prepared by impregnation in boiling ethanol of magnesium basic carbonate with an ammonia solution of copper nitrate.

* Corresponding author. Tel.: +32 4366 3540; fax: +32 4366 3545.
E-mail address: Sophie.Pirard@ulg.ac.be (S.L. Pirard).

1385-8947/$ – see front matter © 2007 Elsevier B.V. All rights reserved.
doi:10.1016/j.cej.2007.06.009

Nomenclature

C	ethylene adsorption constant (atm^{-1})
C_{ref}	preexponential constant of C (atm^{-1})
E_a	activation energy ($J\,mol^{-1}$)
$F_{0.95,a,b}$	Fischer distribution with 95% of confidence, a and b degrees of freedom for the numerator and the denominator of the calculated variable F, respectively
G	free energy ($J\,mol^{-1}$)
H	enthalpy ($J\,mol^{-1}$)
ΔH°	ethylene adsorption enthalpy ($J\,mol^{-1}$)
k	kinetic rate constant ($mol\,min^{-1}\,g^{-1}\,atm^{-1}$)
k_{ref}	preexponential constant of k ($mol\,min^{-1}\,g^{-1}\,atm^{-1}$)
$[L]$	number of active sites on the catalytic surface
n°	sequence number of measurement
$n_{averages}$	number of mean values
n_i	total number of mean values corresponding to temperature i
$n_{measures}$	number of measures including replicates
$n_{parameters}$	number of parameters
n_{points}	number of different measurements in an experimental design; the same number indicates that the measurement is a replicate of the measurements with the same number
O	objective function for the χ^2 test
p_{ij}	weighed factor for experiment corresponding to mean value j and temperature i
P_E	ethylene partial pressure (atm)
P_H	hydrogen partial pressure (atm)
r_s	measured reaction rate ($mol\,min^{-1}\,g^{-1}$)
R	gas constant ($=8.368\,J\,mol^{-1}\,K^{-1}$)
s_e^2	experimental variance ($mol^2\,min^{-2}\,g^{-2}$)
$s_{e,i}^2$	experimental variance for temperature i ($mol^2\,min^{-2}\,g^{-2}$)
s_i^2	residual variance corresponding to model i ($mol^2\,min^{-2}\,g^{-2}$)
S	entropy ($J\,mol^{-1}\,K^{-1}$)
$S^\circ_{C_2H_4}$	standard entropy of ethylene ($J\,mol^{-1}\,K^{-1}$)
ΔS°	ethylene adsorption entropy ($J\,mol^{-1}\,K^{-1}$)
T	temperature (K)
T_{ref}	reference temperature (K)
$\hat{Y}_{ij}$	reaction rate predicted from model 1 and corresponding to temperature i and mean value j and ($mol\,min^{-1}\,g^{-1}$)
$\bar{Y}_{ij}$	mean reaction rate corresponding to temperature i and mean value j ($mol\,min^{-1}\,g^{-1}$)
$\chi^2_{0.95,\nu}$	chi-square distribution with 95% of confidence and ν degrees of freedom
ν	number of degrees of freedom

After impregnation, the mixture was decanted, filtered, washed, and dried. The so-obtained Cu-Mg hydroxycarbonate was then decomposed and activated in Ar flow at 460 °C during 18 h [16,17].

2.2. Experimental setup and procedure

Kinetic data were obtained using a steady state, continuous, differential and isothermal reactor. The reactor was continuously fed with ethylene, hydrogen and argon [16]. Its operating conditions were fixed by adjusting the feed flow rates. By-pass valves allowed to adjust independently the ethylene, hydrogen and argon flow rates. Each experiment lasted 1 h. Among those 60 min, 50 min corresponded to the stabilization phase. Then, the effluent of the reactor was analyzed by gas chromatography using a silicagel column and a hot wire detector. Data were recorded and analyzed during 10 min. Then, the conversion in the reactor was deduced from recorded gas composition.

2.3. Kinetic data acquisition

Several experimental designs were carried out at two temperatures (498 K and 363 K). At first, one octagonal design at 498 K was repeated three times and noted O1–O3, and was supplemented by one octagonal design at 363 K, noted O4. Octagonal design presents the advantage to cover coarsely the whole experimental field. Two additional designs were carried out in order to determine activation energy and thermodynamic adsorption constants. They consisted in changing temperature from 400 to 550 K at the central point of the octagonal design at 498 K, and from 320 to 370 K at the central point of the octagonal design at 363 K. Those two designs were noted Q1 and Q2, respectively.

Subsequently, one sequential design at 498 K, noted S1, and one sequential design at 363 K, noted S2, were performed. Sequential designs were built so as to allow fast discrimination between models or fast parameter estimation by choosing adequate experimental points. The sequential design used the weighted criterion proposed by Hill et al. [24] which is described in Appendix A. That criterion consists in choosing the experimental point which maximizes differences between models and/or gives the best parameter estimation [25]. At first, the reaction rate was measured at three different experimental points which correspond to the central point of octagonal designs and two randomly chosen vertices. Parameters of the competing models (with a number of parameters ≤ 3) were then estimated. Data were analyzed by the sequential design program in order to determine the best next experimental point which discriminates between kinetic models as much as possible and which estimate their parameters with the greater accuracy. Then, reaction rate was measured at this predicted point. A new discrimination, including the new point, between competing models was carried out which could lead to the rejection of some among them. Finally, the last measure and the three previous ones were memorized and the procedure continued by estimating the new best point in the experimental field. The procedure was repeated until the desired precision for model discrimination and parameter estimation was reached.

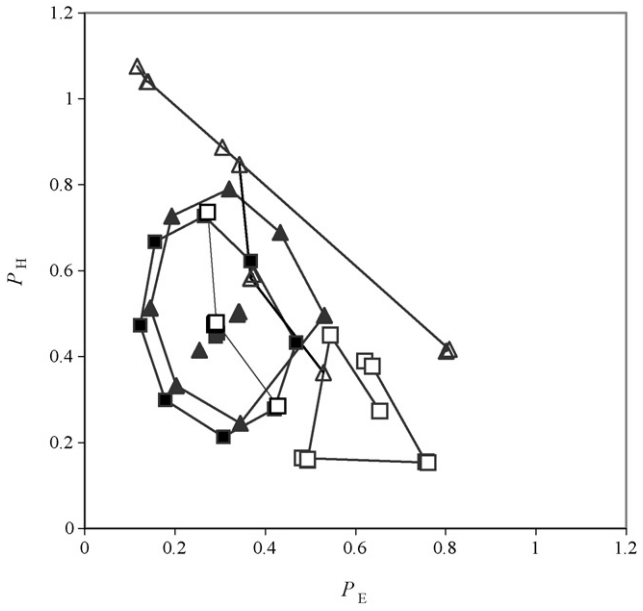

Fig. 1. Representation of octagonal and sequential designs: (■) O1–O3; (▲) O4; (□) S1; (△) S2.

It is important to remark on Fig. 1 that sequential and octagonal designs do not correspond to the same area in the experimental field. Those two approaches (*a priori* octagonal and sequential designs) are compared in Section 4.

3. Results

The experimental reaction rates measured for each experimental design are presented in Tables 1a–1c.

4. Discussion

4.1. Kinetic models

Four phenomenological kinetic rate expressions or models have been studied. Ethane partial pressure does not appear in those rate equations since preliminary experimental measurements highlight that it has no influence on reaction rate [16].

Model 1:

$$r_s = \frac{kCP_E P_H}{1 + CP_E} \quad (1)$$

Model 2:

$$r_s = \frac{kCP_E P_H}{(1 + CP_E)^2} \quad (2)$$

Model 3:

$$r_s = \frac{kCP_E P_H^{1/2}}{1 + CP_E} \quad (3)$$

Model 4:

$$r_s = \frac{kCP_E}{1 + CP_E} \quad (4)$$

Table 1a
Experimental reaction rates for octagonal designs O1–O4

Design	n°	n_{points}	r_s ($\times 10^{-3}$ mol min^{-1} g^{-1})	T (K)	P_E (atm)	P_H (atm)
O1	1	1	4.87	498	0.287	0.451
	2	2	4.30	498	0.147	0.679
	3	3	6.86	498	0.463	0.427
	4	4	6.59	498	0.257	0.741
	5	5	3.99	498	0.424	0.276
	6	1	4.54	498	0.289	0.453
	7	1	4.47	498	0.289	0.454
	8	6	7.38	498	0.354	0.614
	9	7	2.00	498	0.173	0.295
	10	8	2.24	498	0.118	0.474
	11	9	2.12	498	0.305	0.211
	12	1	4.42	498	0.290	0.455
O2	1	1	3.83	498	0.287	0.442
	2	9	1.84	498	0.302	0.209
	3	8	1.92	498	0.120	0.468
	4	7	1.67	498	0.175	0.296
	5	6	6.24	498	0.360	0.613
	6	1	3.83	498	0.289	0.446
	7	1	3.85	498	0.289	0.446
	8	5	3.28	498	0.418	0.275
	9	4	5.20	498	0.261	0.726
	10	3	5.50	498	0.464	0.429
	11	2	3.18	498	0.155	0.666
	12	1	3.55	498	0.291	0.448
	13	1	3.64	498	0.290	0.447
O3	1	1	3.65	498	0.290	0.447
	2	2	3.03	498	0.156	0.667
	3	3	4.98	498	0.468	0.433
	4	4	4.92	498	0.265	0.727
	5	5	3.04	498	0.420	0.278
	6	1	3.36	498	0.295	0.454
	7	1	3.41	498	0.295	0.454
	8	6	5.77	498	0.368	0.622
	9	7	1.55	498	0.178	0.299
	10	8	1.76	498	0.123	0.473
	11	9	1.61	498	0.307	0.213
	12	1	3.41	498	0.295	0.454
	13	1	3.38	498	0.295	0.454
O4	1	1	0.149	363	0.338	0.499
	2	2	0.073	363	0.345	0.245
	3	3	0.144	363	0.145	0.513
	4	4	0.101	363	0.203	0.332
	5	5	0.191	363	0.433	0.689
	6	1	0.141	363	0.341	0.504
	7	1	0.140	363	0.341	0.504
	8	6	0.117	363	0.254	0.415
	9	7	0.215	363	0.320	0.790
	10	8	0.149	363	0.531	0.496
	11	9	0.200	363	0.193	0.727
	12	1	0.142	363	0.342	0.504
	13	1	0.140	363	0.342	0.504

where r_s, P_E, P_H, and C are reaction rate, ethylene and hydrogen partial pressures, and ethylene adsorption constant, respectively. The constant k corresponds to the product of the kinetic constant of rate-determining step and of the hydrogen adsorption constant. On the one hand, model 1 could correspond to a Langmuir–Hinshelwood mechanism with non-competing adsorption of hydrogen and ethylene and where the rate-

Table 1b
Experimental reaction rates for sequential designs S1 and S2

Design	n°	n_{points}	r_s ($\times 10^{-3}$ mol min^{-1} g^{-1})	T (K)	P_E (atm)	P_H (atm)
S1	1	1	3.18	498	0.292	0.477
	2	2	2.93	498	0.428	0.285
	3	3	4.94	498	0.273	0.736
	4	1	3.68	498	0.288	0.474
	5	1	3.56	498	0.289	0.475
	6	4	6.01	498	0.621	0.390
	7	1	3.84	498	0.287	0.473
	8	4	5.73	498	0.637	0.377
	9	5	2.75	498	0.756	0.155
	10	5	2.89	498	0.761	0.153
	11	1	3.64	498	0.289	0.477
	12	6	2.19	498	0.482	0.164
	13	6	2.10	498	0.494	0.158
	14	6	2.11	498	0.494	0.161
	15	7	5.72	498	0.544	0.450
	16	1	3.56	498	0.289	0.475
	17	1	3.55	498	0.292	0.479
	18	8	3.94	498	0.654	0.273
S2	1	1	0.156	363	0.368	0.582
	2	2	0.090	363	0.529	0.363
	3	3	0.209	363	0.343	0.847
	4	1	0.157	363	0.373	0.591
	5	1	0.160	363	0.368	0.582
	6	4	0.250	363	0.138	1.040
	7	1	0.136	363	0.368	0.583
	8	5	0.113	363	0.808	0.417
	9	5	0.108	363	0.801	0.413
	10	4	0.270	363	0.141	1.040
	11	6	0.258	363	0.116	1.076
	12	7	0.231	363	0.305	0.887

Table 1c
Experimental reaction rates for designs varying temperature Q1 and Q2

Design	n°	n_{points}	r_s ($\times 10^{-3}$ mol min^{-1} g^{-1})	T (K)	P_E (atm)	P_H (atm)
Q1	1	1	3.55	500	0.287	0.443
	2	2	3.41	489	0.289	0.444
	3	3	3.18	476	0.291	0.446
	4	4	2.71	462	0.295	0.449
	5	5	2.11	440	0.302	0.456
	6	6	1.27	421	0.310	0.462
	7	7	0.61	401	0.316	0.467
	8	8	0.27	384	0.319	0.469
	9	9	3.61	512	0.286	0.442
	10	10	3.59	521	0.286	0.442
	11	11	3.63	535	0.286	0.442
	12	12	3.58	550	0.286	0.442
Q2	1	1	0.152	369	0.346	0.510
	2	2	0.095	360	0.346	0.510
	3	3	0.063	351	0.346	0.510
	4	4	0.047	345	0.346	0.510
	5	5	0.030	338	0.346	0.510
	6	6	0.019	330	0.346	0.510
	7	7	0.013	325	0.346	0.510
	8	8	0.019	332	0.346	0.510
	9	9	0.029	340	0.346	0.510
	10	10	0.043	346	0.346	0.510
	11	11	0.060	352	0.346	0.510
	12	12	0.097	360	0.346	0.510
	13	13	0.163	371	0.346	0.510

determining step is either the addition of molecularly adsorbed hydrogen or the addition of the second atom of hydrogen adsorbed dissociatively. In such a case, the hydrogen adsorption should be weak enough to be neglected. On the other hand, model 1 could also correspond to an Eley-Rideal mechanism in which gaseous hydrogen would be directly added on adsorbed ethylene. Model 2 corresponds to competitive adsorption of both reactants. The rate-determining step is either the addition of molecularly adsorbed hydrogen or the addition of the second atom of hydrogen adsorbed dissociatively. Model 3 is characterized by a non-competitive adsorption of ethylene and hydrogen, and by an atomic mechanism for which the addition of the first hydrogen atom to adsorbed ethylene is the rate-determining step. For those two last models, it is supposed that hydrogen adsorption is very weak. As far as the fourth model is concerned, it corresponds to a mechanism characterized by a non-competitive adsorption of reactants and by a hydrogen adsorption independent of hydrogen partial pressure due to strong hydrogen adsorption. While unlikely, that model has been retained so as to test the design of experiments. It has to be mentioned that more rate equations are phenomenologically possible for rather simple hydrogenation reaction of ethylene, but these can be excluded on the basis of the obtained results.

4.2. Discrimination between kinetic models

The first part of the study consists in the discrimination between those four models. With this intention, parameter estimation was performed with each model and for each experimental design. The software used is derived from NLPE program. The Gauss–Newton method was used to optimize the parameters [26]. A maximum likelihood formulation was adopted, thus minimizing the weighed sum of squares of the differences between calculated and measured reaction rates. The experimental variances used as weight were estimated from replicated measurements. It has to be noted that this analysis assumes that all points have the same weight, thus the measurement variance is constant. Results are presented in Table 2. Each parameter is given with its 95% confidence interval calculated from the *t*-Student test [25,27–29].

4.2.1. Study of octagonal designs

The first step consists in considering results of *F*-tests realized on octagonal designs [25,27–29]. With octagonal designs O1–O4, the number of observations is equal to 13 and the number of degrees of freedom, ν, is therefore equal to $13 - 2 = 11$. Concerning octagonal designs at 498 K (O3), the ratio between residual variances of models 3 and 1 (13.4) is larger than the $F_{0.95,11,11}$ variable (2.82), which means that model 3 and *a fortiori* model 4 do not fit data as well as model 1. Indeed, the residual variance corresponding to model 4 (1.2) is larger than the residual variance corresponding to model 3 (0.27). Thus the ratio of the residual variances corresponding to models 4 and 1 (60) is larger than the variable $F_{0.95,11,11}$ (2.82). On the contrary, the sum of squares of residuals for models 1 and 2 are identical. Therefore, those two models cannot be discriminated at 498 K ($s_2^2/s_1^2 = 1 < F_{0.95,11,11} = 2.82$).

Table 2
Parameter estimation with Eqs. (1)–(4) with each experimental design separately

Design	$k' = kC$ ($\times 10^{-3}$ mol min^{-1} g^{-1} atm^{-2})	k ($\times 10^{-3}$ mol min^{-1} g^{-1} atm^{-1})	C (atm^{-1})
			*Model*1
O1	41 ± 5	[a]	0.49 ± 0.44
O2	32 ± 3	[a]	0.33 ± 0.30
O3	30 ± 3	[a]	0.49 ± 0.32
S1	27 ± 2	[a]	0.22 ± 0.18
O4	[b]	0.27 ± 0.01	[c]
S2	[b]	0.27 ± 0.01	[c]
			*Model*2
O1	40 ± 5	[a]	0.22 ± 0.20
O2	31 ± 3	[a]	0.15 ± 0.14
O3	30 ± 3	[a]	0.22 ± 0.14
S1	27 ± 2	[a]	0.10 ± 0.08
O4	[b]	[c]	[c]
S2	[b]	[c]	[c]
			*Model*3
O1	36 ± 16	[a]	[c]
O2	27 ± 9	[a]	[c]
O3	25 ± 10	[a]	[c]
S1	29 ± 8	[a]	2.0 ± 1.5
O4	[b]	[c]	[c]
S2	[b]	0.22 ± 0.06	[c]
			*Model*4
O1	[c]	[a]	[c]
O2	21 ± 19	[a]	[c]
O3	19 ± 19	[a]	[c]
S1	[c]	[a]	[c]
O4	[b]	[c]	[c]
S2	[b]	0.18 ± 0.07	[c]

[a] Parameter k not adjusted (product kC replaced by k' for parameter estimation).
[b] Parameter k' not adjusted (product kC retained for parameter estimation).
[c] Parameter impossible to adjust precisely and non-significantly different from 0.

At 363 K, the F-test realized on the octagonal design O4 leads to the conclusion that models 2–4 can be eliminated ($s_2^2/s_1^2 = 900$, $s_3^2/s_1^2 = 12$, $s_4^2/s_1^2 = 59 > F_{0.95,11,11} = 2.82$).

Those two statistical tests lead to the elimination of models 2–4. Model 1 is the only one able to fit all experimental data at 363 and 498 K. Between competitive or non-competitive mechanisms, and hydrogen order 1 (non-adsorbed or molecularly adsorbed H_2 addition as rate-determining step or dissociative adsorption with addition of the second H as rate-determining step) or order 1/2 (dissociative adsorption with addition of the first H) proposed in literature [1,19,20,22,23], the present statistical study thus concludes that ethylene hydrogenation on a Cu-MgO catalyst occurs *via* a non-competitive mechanism with order 1 for hydrogen, the latter being non or very weakly adsorbed.

4.2.2. Study of sequential designs

Subsequently, sequential designs are considered. Sequential designs are built to allow fast discrimination between models or fast precise parameter estimation by choosing adequate experimental points. Five successive experimental points at 498 K and four successive points at 363 K were calculated from the three points initially chosen. Successive parameter estimations were performed by adding one by one the calculated points. Results are presented in Table 3. It must be noted that parameter C, estimated for each model, is not significantly different from zero whatever the number of points considered. That is the reason why this parameter is not specified in Table 3. Several conclusions can be drawn. The discrimination between models at 498 K (S1) indicates that only four experiments, which correspond to one point added, allow to reject models 3 and 4 on the basis of the F-test. On the contrary, models 1 and 2 cannot be discriminated. It is true whatever the number of observations. At 363 K (S2), the addition of only one point allows to reject all models except model 1. Concerning parameter estimation, it is observed that the addition of a single experiment ($n_{points} = 4$) allows to reach the best precision. The addition of next points in S1 for models 1 and 2 and in S2 for model 1 does not improve the knowledge of parameters. The conclusion is that the four first experimental points only were necessary in S1 and S2.

4.2.3. Simplification of model 1

It is important to note that the constant C cannot be adjusted precisely at 363 K for the first model (Table 2). Indeed, ethylene adsorption becomes stronger at low temperature, which results in the increase of C in (1). Therefore, the term 1 of the denominator becomes negligible. In others words, at low temperature, kinetic

Table 3
Parameter estimation with Eqs. (1)–(4) and F-test for sequential designs by adding one by one points calculated by the sequential design[d]

Design	n_{points}	$k' = kC$ ($\times 10^{-3}$ mol min^{-1} g^{-1} atm^{-2})	k ($\times 10^{-3}$ mol min^{-1} g^{-1} atm^{-1})	$\frac{s^2_{i,n_{points}}}{s^2_{1,n_{points}}}$	$F_{0.95,n_{points}-2,n_{points}-2}$
S1					
Model 1	3	28 ± 22	[a]	1	161
	4	27 ± 2	[a]	1	19
	5	27 ± 2	[a]	1	9
	6	27 ± 2	[a]	1	6
	7	27 ± 2	[a]	1	5
	8	27 ± 2	[a]	1	4
Model 2	3	28 ± 20	[a]	1	161
	4	27 ± 2	[a]	1	19
	5	27 ± 2	[a]	1	9
	6	27 ± 2	[a]	1	6
	7	27 ± 2	[a]	1	5
	8	28 ± 2	[a]	1	4
Model 3	3	[c]	[a]	6	161
	4	[c]	[a]	31	19
Model 4	3	[c]	[a]	140	161
	4	[c]	[a]	1200	19
S2					
Model 1	3	[b]	[c]	1	161
	4	[b]	0.26 ± 0.02	1	19
	5	[b]	0.27 ± 0.02	1	9
	6	[b]	0.27 ± 0.02	1	6
	7	[b]	0.27 ± 0.02	1	5
Model 2	3	[b]	[c]	156	161
	4	[b]	[c]	30500	19
Model 3	3	[b]	[c]	4	161
	4	[b]	[c]	84	19
Model 4	3	[b]	[c]	16	161
	4	[b]	[c]	400	19

[a] Parameter k not adjusted (product kC replaced by k' for parameter estimation).
[b] Parameter k' not adjusted (product kC retained for parameter estimation).
[c] Parameter impossible to adjust precisely.
[d] When the model is eliminated, the parameter estimation is not performed.

Eq. (1) simplifies in

$$r_s = kP_H \quad (5)$$

The only parameter is the kinetic constant k. This is the reason why the constant C is badly known. At high temperature, the very weak value of C leads to neglect the term CP_E of the denominator, and the kinetic equation simplifies in

$$r_s = kCP_E P_H = k' P_E P_H \quad (6)$$

In this case, k and C are completely correlated. Only their product $k' = kC$ can be precisely estimated.

4.2.4. Sequences of elementary steps

Octagonal designs as well as sequential designs reject all models proposed, except model 1. The three sequences of elementary steps corresponding to model 1 are thus:

Sequence 1	$C_2H_4 + \underline{s_1} \leftrightarrow \underline{C_2H_4 - s_1}$ $H_2 + \underline{s_2} \leftrightarrow \underline{H_2 - s_2}$ $\underline{C_2H_4 - s_1} + \underline{H_2 - s_2} \rightarrow$
Sequence 2	$C_2H_4 + \underline{s_1} \leftrightarrow \underline{C_2H_4 - s_1}$ $H_2 + 2\underline{s_2} \leftrightarrow 2\underline{H - s_2}$ $\underline{C_2H_4 - s_1} + \underline{H - s_2} \leftrightarrow \underline{C_2H_5 - s_1} + \underline{s_2}$ $\underline{C_2H_5 - s_1} + \underline{H - s_2} \rightarrow$
Sequence 3	$C_2H_4 + \underline{s} \leftrightarrow \underline{C_2H_4 - s}$ $\underline{C_2H_4 - s} + H_2 \rightarrow$

The two first sequences of elementary steps correspond to a Langmuir–Hinshelwood mechanism, while the last sequence of elementary steps corresponds to an Eley-Rideal mechanism, as explained in Section 4.1.

4.3. Catalyst deactivation

From a quantitative point of view, the comparison between values of parameter k at 363 K for O4 and S2 highlights

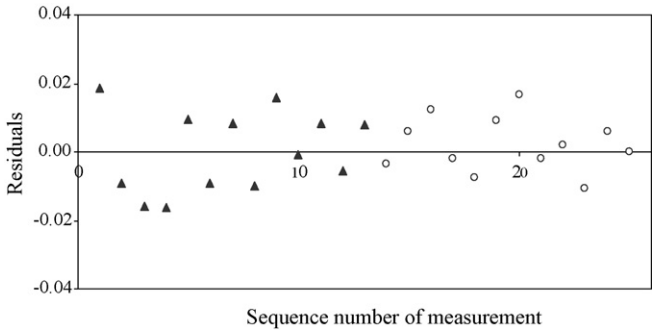

Fig. 2. Residuals of parameter estimation ((▲) O4; (◯) S2) as a function of sequence number of measurement.

the perfect agreement between those two designs (Table 2: $k = 0.27 \times 10^{-3}$ mol min^{-1} g^{-1} atm^{-1}). Fig. 2 gathers residuals of octagonal and sequential designs at 363 K, as a function of the sequence number of measurement. Ideally, residuals should be distributed randomly which is the case for Fig. 2. On the contrary, some differences can be underlined at 498 K: the constant k' is slightly different for the four designs performed at that temperature. The reason for this discordance is the decrease of catalytic activity between each experimental design, while the very slight decrease of catalytic activity can be neglected inside each design. The decrease of catalytic activity level results from the decrease of the number of active sites on the catalytic surface. That is the reason why the parameter k' decreases when moving from design O1 to designs O2, O3 and S1 (from 41×10^{-3} to 27×10^{-3} mol min^{-1} g^{-1} atm^{-2}). This problem must be solved in order to determine the correct values of parameters. A correction of reaction rates taking catalytic deactivation into account is necessary in order to obtain the same activity level for each experimental data so that confidence ellipses of parameters will become centered on the same point. The octagonal design O3 is chosen to be the reference for the activity level. Initial rates are corrected by dividing them by the value of k' in model 1 obtained from the corresponding design, and by multiplying them by the value of k' corresponding to O3, *i.e.* 30×10^{-3} mol min^{-1} g^{-1} atm^{-2}. Values obtained for k' are identical for the four designs, but the parameter C does not differ significantly from zero. The simplified Eq. (6) of model 1 should therefore be used for correction, by using the k' values obtained from parameter estimation with this simplified model.

The activity level correction procedure consists in introducing a third parameter $[L]$ in model 1, corresponding to the number of active sites on the catalytic surface. Therefore, model 1 can be represented by Eq. (7):

$$r_s = \frac{[L]kCP_E P_H}{1 + CP_E} = \frac{[L]k'P_E P_H}{1 + CP_E} \quad (7)$$

The parameter $[L]$ is adjusted for each design by dividing the value of k' of the corresponding design by the value of k' corresponding to O3 and by taking $[L] = 1$ for the reference design O3. It has to be noted that at 363 K, $[L] = 1$ for both the octagonal design O4 and the sequential design S2 because k is the same for those two designs (Table 2), which thus correspond to the same activity level.

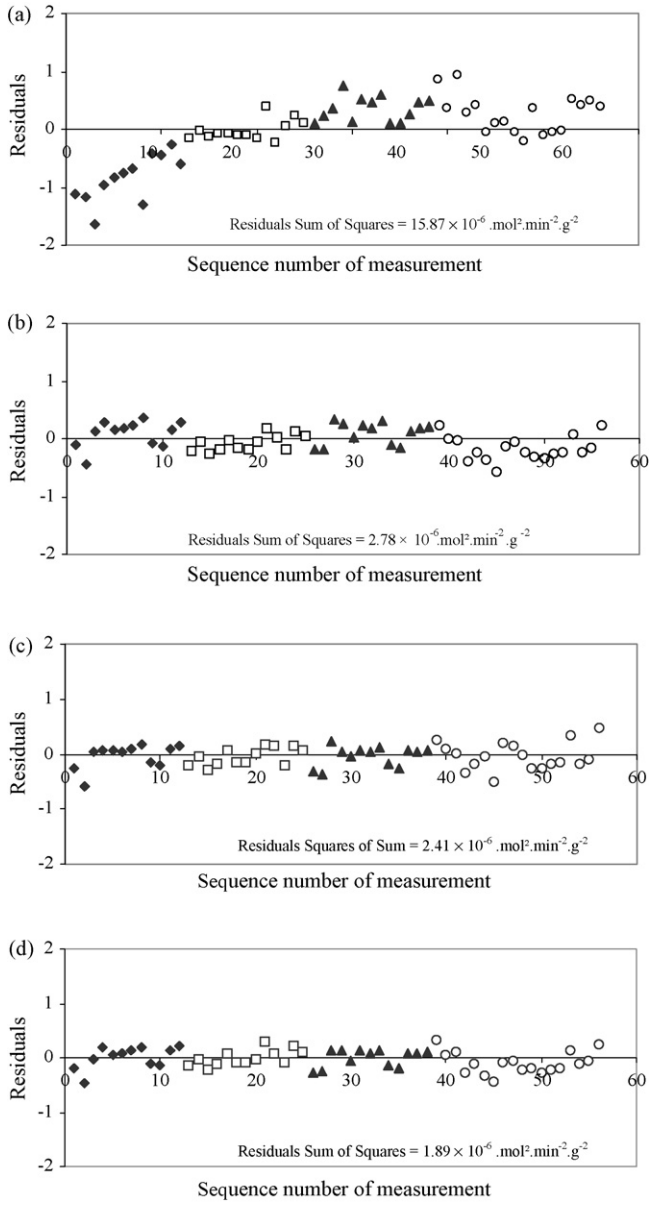

Fig. 3. Residuals of parametric adjustment ((♦) O1; (□) O2; (▲) O3; (◯) S1) as a function of sequence number of measurement (a) on the non-simplified model 1 without any correction on initial reaction rate; (b) on the non-simplified model 1 after rate correction on the non-simplified model 1; (c) on the simplified model 1 after rate correction on the simplified model 1; (d) on the non-simplified model 1 after rate correction on the simplified model 1.

Fig. 3 illustrates the evolution of the rate correction procedure by means of residuals maps corresponding to parameter estimation of model 1 with the four designs at 498 K. Ideally, residuals must be distributed randomly and the residuals sum of squares must be as small as possible, which is the case after the final correction (Fig. 3(d)). The residuals sum of squares quantifies the benefit of taking catalytic deactivation into account. Furthermore, Fig. 5(a) shows that the confidence ellipses of parameters are centered on the same point.

It has to be noted that another way to correct reaction rates in order to obtain the same activity level consists in calculating one mean value for the central point of the three octagons O1–O3.

One mean value is also calculated for the sequential design S1 on the experimental point corresponding to the central point of the octagon at 498 K, repeated seven times in design S1 and corresponding to the n_{points} equal to 1 in Table 1b. Then, reaction rates are corrected by dividing them by the mean value of the corresponding design and by multiplying them by the mean value corresponding to design O3. This kind of correction consists in determining parameter $[L]$ for each design by dividing the mean value of the corresponding design by the mean value corresponding to design O3. While correction from mean values at the central point of octagons is easier, correction from k' obtained by parameter estimation with non-corrected data allows to take deactivation over all experimental field into account. Results provided by those two methods do not differ in this study.

As a conclusion of this paragraph, parameter estimation of model 1 can be divided into two steps. The first step consists in the determination of the parameter $[L]$ which quantifies catalytic deactivation, while the second step results in the estimation of the two parameters k' and C. So two successive adjustments are carried out.

4.4. Temperature dependent model

Model 1 can be refined by taking into account temperature. This involves the knowledge of the temperature dependence of parameters k and C. The rate constant k is developed according to Arrhenius law, while the ethylene adsorption constant C follows van't Hoff's law [27]:

$$k = k_{ref} \exp\left[-\frac{E_a}{R}\left(\frac{1}{T} - \frac{1}{T_{ref}}\right)\right] \quad (8)$$

$$C = C_{ref} \exp\left[-\frac{\Delta H^\circ}{R}\left(\frac{1}{T} - \frac{1}{T_{ref}}\right)\right] \quad (9)$$

where E_a, ΔH°, C_{ref}, k_{ref} and T_{ref}, are, respectively, the activation energy, the adsorption enthalpy, the preexponential constant of C, the preexponential constant of k and a reference temperature which is intermediate between 363 and 498 K and chosen equal to 450 K. In order to answer later the question of knowing which designs are really necessary, several parameter estimations as a function of temperature have been performed with different experimental designs according to Fig. 4. First, one octagonal design at 498 K (O3) and one octagonal design at 363 K (O4) were only considered. It corresponds to adjustment (i). Secondly, in order to underline the influence of additional non-isothermal data on the results, two designs with varying temperatures Q1 and Q2 were added and this corresponds to adjustment (iii). Finally, the two sequential designs S1 and S2 were added, which corresponds to adjustment (v). The influence of replicates was studied by adding the two other octagonal designs O1 and O2 at 498 K to those three groups of data. The corresponding adjustments are (ii), (iv) and (vi), respectively. Furthermore, the two sequential designs S1 and S2 were tested separately from other designs, and compared to adjustments (i) and (ii). This adjustment is noted (vii). Then, the two designs with varying temperature, Q1 and Q2, were added to sequential designs in order to compare with adjustments (iii) and (iv). This group of data is noted (viii).

It is important to note that experimental variance has not been kept constant at all temperatures. Observations were replicated at 363 and 498 K to allow estimation of experimental variance, whose inverse is used as a weight in the objective function to be optimized. That is the reason why all experimental data can be treated simultaneously. Results are presented in Table 4. Several conclusions can be drawn. First, the two octagonal designs at 498 and 363 K, corresponding to adjustment (i), are not sufficient to estimate adsorption parameters, C_{ref} and ΔH°, with acceptable precision. With the two sequential designs corresponding to adjustment (vii), three parameters, k_{ref}, C_{ref} and ΔH°, are only coarsely estimated. Secondly, the addition of designs Q1 and Q2 to the two octagonal designs, *i.e.* adjustment (iii), brings much more information on temperature dependence, and all four parameters are better known. Parameter uncertainty is also reduced when Q1 and Q2 are added to S1 and S2, corresponding to adjustment (viii), compared with adjustment (vii). On the other hand, the addition of sequential designs to adjustment (iii), which corresponds to adjustment (v), does not significantly improve the knowledge of parameters. Furthermore, the addition of O1 and O2 to adjustments (i), (iii) and (v), which corresponds to adjustments (ii), (iv) and (vi), respectively, does not lead to a reduction of parameter uncertainty. So designs O1 and O2 are useless.

The last step consists in determining the ethylene adsorption entropy ΔS°. By introducing the van't Hoff's law (Eq. (10)) [27] and the Gibbs' free energy (Eq. (11)) into Eqs. (1), (8) and (9), the adsorption entropy is related to the four parameters k_{ref}, C_{ref}, E_a and ΔH° by Eq. (12) and its estimation value is equal to $-133 \pm 8\ \mathrm{J\,mol^{-1}\,K^{-1}}$.

$$C = \exp\left(-\frac{\Delta G^\circ}{RT}\right) \quad (10)$$

$$G = H - TS \quad (11)$$

$$\Delta S^\circ = R \ln C_{ref} + \frac{\Delta H^\circ}{T_{ref}} \quad (12)$$

Let us mention that ethylene adsorption enthalpy and entropy, ΔH° and ΔS°, must verify thermodynamic constraints. Indeed, adsorption is an exothermic process with decreasing entropy [30]:

$$\Delta H^\circ < 0 \quad (13)$$

$$0 < -\Delta S^\circ < S^\circ_{C_2H_4} = 220\ \mathrm{J\,mol^{-1}\,K^{-1}} \quad (14)$$

Values of ΔH° and ΔS° obtained here are in agreement with those constraints.

4.5. Which is the minimum set of observations required?

Several parameter estimations have been performed with different experimental designs at 498 K in order to determine the constant k' with a precision as good as possible. Fig. 5(a) shows the precision improvement for k' at 498 K. The simultaneous treatment of the three octagonal designs improves very slightly

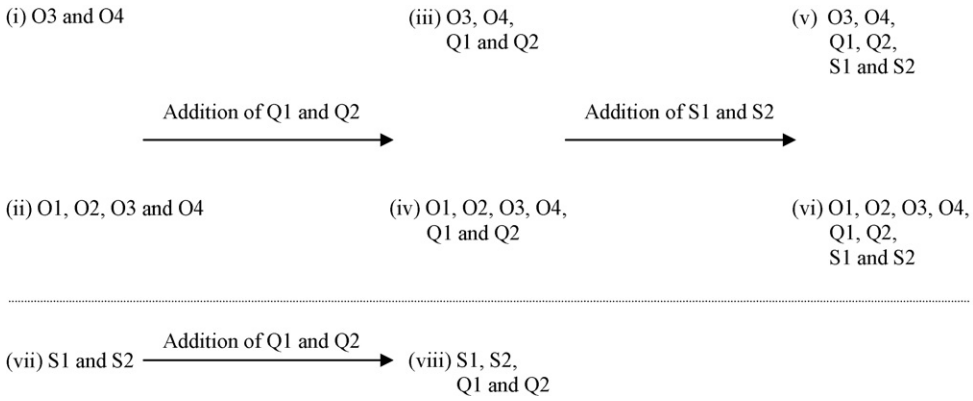

Fig. 4. Diagram representing the different data groups for parameter estimation.

the knowledge of k', in the same way that the simultaneous treatment of one octagonal design and one sequential design, while the addition of the sequential design to the three octagonal designs reduces very few the confidence interval of this parameter. So, it was not necessary to complete three octagonal designs and one sequential design. Indeed, one octagonal design and one sequential design are sufficient to lead to a very good precision. At 363 K, the sequential design S2 and the octagonal design O4 lead to the same precision of the parameter k, as shown in Fig. 5(b). Fig. 5(b) represents the confidence interval of parameter k at 363 K, for designs O4 and S2 separately and designs O4 and S2 together. The addition of those two designs does not lead to an actual improvement of the knowledge of k. Nevertheless, as shown in Table 3, whatever the temperature, the four first observations of sequential designs are sufficient to obtain the same precision as with octagonal designs, and the following observations of sequential designs do not lead to a precision improvement. So the sequential design leads faster to a good parameter estimation and should be used preferentially. Furthermore, sequential design makes possible to set the minimum amount of experiments before performing too many experiments. Indeed, sequential design is built from three initial points by adding new points one by one, making possible to freely stop experiments when parameter estimation is good enough and model discrimination successfully performed. This is not possible for octagonal design which is built *a priori*. So only sequential designs allow to limit experimental efforts.

By examining results in Table 4 corresponding to adjustments as a function of temperature, the addition of the two first octagonal designs O1 and O2 to adjustments (i), (iii) and (v), which corresponds to adjustments (ii), (iv) and (vi), respectively, does not lead to a better precision. From this point of view, O1 and O2 are useless. Furthermore, parameter estimations with sequential designs, S1 and S2, and designs with varying temperature, Q1 and Q2, which corresponds to adjustment (viii), gives also a very precise estimation of parameters, which is similar to precision obtained with adjustment (iii) including O3, O4, Q1 and Q2. Furthermore, the addition of sequential designs to adjustments (iii) and (iv), which corresponds to adjustments (v) and (vi), respectively, very slightly improves the parameter knowledge. So, in this case, the use of all experimental designs is necessary only if a very good parameter precision is required. In practice however, O3, O4, Q1 and Q2 or S1, S2, Q1 and Q2 are sufficient.

Now the question of knowing which designs are really necessary can be answered. If the two designs Q1 and Q2 with varying temperature are obviously necessary to determine the five parameters [L], k_{ref}, C_{ref}, E_a and ΔH°, only one octagonal design at 498 K (O3) and one at 363 K (O4), or one sequential design at 498 K (S1) and one sequential design at 363 K (S2), are enough to obtain a good precision of parameters. However, the simultaneous treatment of sequential and octagonal designs allows to reach a slightly better precision. In fact, experimental points corresponding to sequential designs sweep another area of the experimental field than the area spanned by octagonal designs. So the treatment of all experimental data, from sequential and octagonal designs, provides more precision resulting from more different experimental conditions. As a conclusion, it can be stated that sequential designs allow to reach a good

Table 4
Kinetic and thermodynamic parameters, standard error and residual variances for model 1 and for each data group

	k_{ref} ($\times 10^{-3}$ mol min^{-1} g^{-1} atm^{-1})	C_{ref} (atm^{-1})	E_a (kJ mol^{-1})	ΔH° (kJ mol^{-1})
i	13 ± 4	[a]	61 ± 5	[a]
ii	16 ± 7	[a]	64 ± 3	[a]
iii	11 ± 2	2.9 ± 1.0	60 ± 3	−61 ± 2
iv	13 ± 3	2.4 ± 0.9	61 ± 4	−62 ± 3
v	15 ± 3	1.8 ± 0.5	64 ± 3	−62 ± 3
vi	15 ± 3	2.0 ± 0.5	63 ± 3	−62 ± 3
vii	20 ± 8	1.5 ± 1.4	68 ± 6	−72 ± 3
viii	15 ± 3	1.9 ± 0.6	64 ± 3	−63 ± 3

[a] Parameter impossible to adjust with precision.

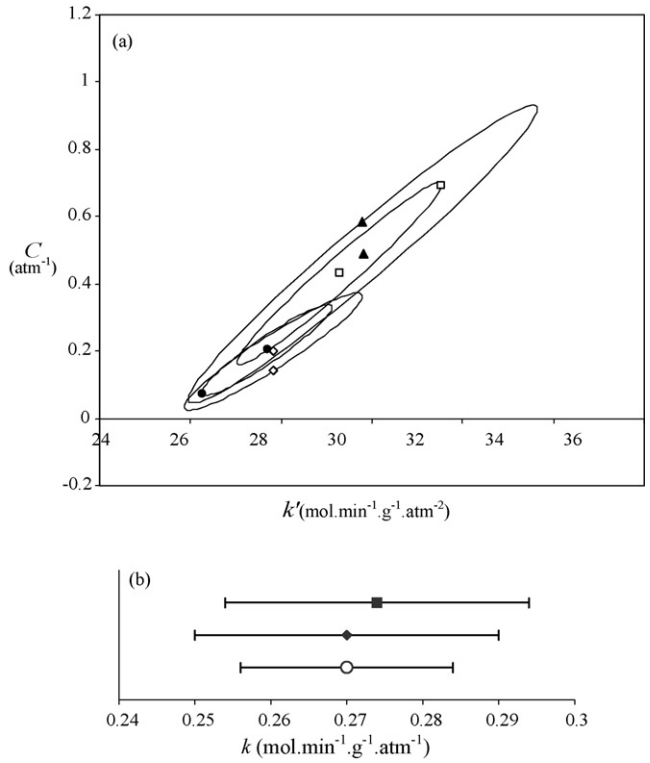

Fig. 5. (a) Confidence ellipses at 498 K for designs (▲) O3; (□) O1–O3; (◊) O3 and S1; (●) O1–O3 and S1. (b) Interval of confidence of k at 363 K: (■) O4; (♦) S2; (◯) O4 and S2.

precision more rapidly, to discriminate between kinetic models more rapidly, and to limit experimental efforts. If the precision required is not reached, experimental points in another area of experimental conditions must be performed.

4.6. Checking of catalytic activity level

Data obtained from the three octagonal designs at 498 K have been corrected to correspond to the same activity level, that is the reference level of O3 (see Section 4.3). However, the equality between activity levels at 498 K and 363 K has still to be checked. Because the temperature dependence of the parameter k is known (Eq. (9)), the idea is to calculate the constant k_{ref} again, from the value of k and k' obtained at 363 K and 498 K, respectively. The two values of k_{ref} at 363 K (15.0) and at 498 K (14.7) are not significantly different. They prove the good agreement between the activity levels at both temperatures.

4.7. Experimental error and validation of model 1

The experimental error at 363 and 498 K has been calculated in order to validate model 1 by performing a F-test [25,28,29]. This test compares the experimental variance and the residual variance of model 1. Because the octagonal design at 498 K was repeated three times, it is possible to calculate an experimental variance s_e^2 at 498 K. Two different experimental variances can be calculated. The first experimental variance results from all the points of O1, O2 and O3, by calculating nine averages, *i.e.* one average on three points at each vertex of the octagon, and one average at the central point of the octagon repeated four times for O1 and five times for O2 and O3. The number of degrees of freedom ν and the corresponding experimental variance s_e^2 are equal to $(12+13+13-9)=29$ and $0.02\times10^{-6}\,\mathrm{mol^2\,min^{-2}\,g^{-2}}$, respectively. The second experimental variance at 498 K considers that the octagonal designs O1–O3 are three different designs with the same central point, on which the experimental variance is calculated. This second experimental variance is equal to $0.02\times10^{-6}\,\mathrm{mol^2\,min^{-2}\,g^{-2}}$, with $(4+5+5-1)=13$ degrees of freedom. At 363 K, the experimental variance s_e^2 is calculated from the central point of the octagon repeated five times, and is equal to $10^{-5}\times10^{-6}\,\mathrm{mol^2\,min^{-2}\,g^{-2}}$, with $(5-1)=4$ degrees of freedom.

The F-test was performed on the octagonal design O4 at 363 K and on the three octagonal designs O1–O3 at 498 K. For the latter temperature, two tests were performed which use the two experimental variances from the two methods explained above. For each temperature, the residual variance of the model 1 is not significantly different from experimental variance (O4 : $s_1^2/s_e^2 = 3.0 < F_{0.95,7,4} = 6.1$, *i.e.* $s_1^2 \cong s_e^2$; O1–O3 with only one average: $s_1^2/s_e^2 = 1.4 < F_{0.95,22,13} = 2.4$, *i.e.* $s_1^2 \cong s_e^2$; O1–O3 with one average for each points of the octagon: $s_1^2/s_e^2 = 2.3 < F_{0.95,6,29} = 2.4$, *i.e.* $s_1^2 \cong s_e^2$). Results of F-tests allow to validate model 1 for both temperatures.

If F-tests validate model 1 at 363 K and at 498 K separately, model 1 as a function of temperature has yet to be validated. With this intention, a χ^2 test [25,29] was performed on the four octagonal designs O1–O4, and on the two designs Q1 and Q2 with varying temperature. This statistical test takes the fact that experimental variances are different at 363 K and at 498 K into account. Because no repetition were performed for the two designs Q1 and Q2 with varying temperature, it is supposed that the experimental variance corresponding to Q1 is equal to the experimental variance at 498 K, and that the experimental variance corresponding to Q2 is equal to the experimental variance at 363 K. According to χ^2 test, model 1 is validated if the calculated objective function O is smaller than the variable χ^2 for the corresponding degrees of freedom ν. The objective function corresponds to the sum of squares of residuals standardized by the adequate experimental variance.

$$O = \sum_{i=1}^{2}\sum_{j=1}^{n_i} p_{ij}\left[\frac{(\bar{Y}_{ij}-\hat{Y}_{ij})}{s_{e,i}}\right]^2 \tag{15}$$

In Eq. (15), the subscript i corresponds to the temperature. i equal to 1 corresponds to 498 K and design Q1, while i equal to 2 corresponds to 363 K and design Q2. The subscript j refers to the number of means calculated for each temperature. n_i is the total number of mean values calculated for each temperature and p_{ij} is the weight attributed to each mean. In the case where experimental variance at 498 K is calculated only with the central point of the octagon repeated 14 times, $n_1 = 50-(14-1)=37$ and $n_2 = 26-(5-1)=22$.

Furthermore, the numbers of degree of freedom corresponding to $s_{e,1}^2$ and $s_{e,2}^2$ are equal to $(14-1)=13$

and $(5-1)=4$, respectively. In the case where experimental variance is calculated with the 38 points of O1–O3, $n_1=50-(14-1)-(3-1)\times 8=21$ and $n_2=26-(5-1)=22$.

Furthermore, the numbers of degrees of freedom corresponding to $s^2_{e,1}$ and $s^2_{e,2}$ are equal to $((12+13+13)-9)=29$ and $(5-1)=4$, respectively. The variable $\chi^2_{0.95,\nu}$ depends on the degrees of freedom. Seventy six measurements corresponding to O1–O4, Q1 and Q2 are included in this adjustment on model 1 belonging five parameters $[L]$, k_{ref}, C_{ref}, ΔH° and E_a. In the case where experimental variance at 498 K is calculated only with the central point of the octagon, the number of degrees of freedom is equal to $(50-((5+5+4)-1)+26-(5-1)-5)=53$. The objective function was found to be equal to 37, while $\chi^2_{0.95,53}$ is greater and equal to 71 with a probability of 95%. So model 1 is validated as a function of temperature. In the second case where experimental variance is calculated with the 38 points of O1–O3, the number of degrees of freedom is equal to $(50-((5+5+4)-1)-(8\times(3-1))+26-(5-1)-5)=38$. The objective function was found to be equal to 48, while $\chi^2_{0.95,38}$ is greater and equal to 53 with a probability of 95%. So model 1 is also validated as a function of temperature with this second $\chi^2_{0.95,\nu}$ test.

4.8. Comparison with previous literature

Model 1 has been found to be the best model in agreement with experimental data and has been validated with experimental data. Parameter estimation provides an activation energy equal to $64\pm 3\,kJ\,mol^{-1}$, while ethylene adsorption enthalpy and entropy are equal to $-63\pm 3\,kJ\,mol^{-1}$ and $-133\pm 8\,J\,mol^{-1}\,K^{-1}$, respectively. Activation energies given in previous literature for ethylene hydrogenation on copper at temperatures between 273 and 523 K, which contains roughly the range examined here, are between 29 and $55\,kJ\,mol^{-1}$ [16,21]. The rate of ethylene hydrogenation on copper–nickel alloy films in the temperature range 0–21 °C was also measured [31]. The apparent energies of activation for the reaction over the copper–nickel alloys vary with composition in the range 38–50 $kJ\,mol^{-1}$, while the apparent activation energies over gold–nickel alloys are about $17\,kJ\,mol^{-1}$. Concerning ethylene hydrogenation on other metal-supported catalysts, Hirschl et al. [32] performed a density-functional study for hydrogenation of ethylene on Pt(1 1 1) and $Pt_{80}Fe_{20}$(1 1 1) and they obtained an activation energy equal to 77 and $67\,kJ\,mol^{-1}$, respectively. In the same way, Duca et al. [33] combined kinetic and thermodynamic methods to mimic surface reactions and reported Arrhenius plot for the hydrogenation of ethylene on Pt/silica catalysts. They related an activation energy equal to $67\pm 8\,kJ\,mol^{-1}$, in agreement with Hirschl et al. Concerning supported Pd catalysts, the apparent activation energy for ethylene hydrogenation decreases with increasing temperature and experimentally reported values range from 25 to $45\,kJ\,mol^{-1}$ when temperature varies from 436 to 248 K [1,34–40]. It can be concluded that activation energy obtained in this study is in the same order of magnitude comparing to values related to ethylene hydrogenation on different kind of catalysts. Finally, on metals from group VIII, the activation energy of ethylene hydrogenation most of the time is contained between 30 and $45\,kJ\,mol^{-1}$ [20,21]. Those values were determined at very different temperatures contained between 153 and 873 K. In the particular case of palladium, values of $35\,kJ\,mol^{-1}$ (for temperatures around 243 K), $31\,kJ\,mol^{-1}$ ($343\,K\le T\le 403\,K$), and $23\,kJ\,mol^{-1}$ ($273\,K\le T\le 373\,K$) were reported. On silver, a much higher activation energy of $113\,J\,kJ\,mol^{-1}$ was obtained for ethylene hydrogenation between 823 and 973 K [21].

Comparisons can also been made concerning kinetic reaction orders. This study performed on a Cu-MgO catalyst determines model 1 as the best model able to fit with experimental data. This model corresponds to an ethylene order varying from 0 to 1, while hydrogen order is equal to 1. In experimental studies on Pt, the kinetic reaction orders vary from 0.5 to 1 in hydrogen and from slightly negative to slightly positive in ethylene [41,42]. Concerning Pd catalysts, the hydrogen order is around 0.8 and the ethylene order varies from −0.2 to 0 [34]. Over copper–nickel alloys, the reaction rate is first order with respect to hydrogen and independent of ethylene for the copper–nickel alloys and for pure nickel. It is first order with respect to both hydrogen and ethylene for copper catalysts. Those results are in good agreement with the hydrogen partial order value obtained in the present study, while they are compatible with the ethylene partial order value obtained in this study and ranging between 0 and 1.

5. Conclusion

The kinetic study of ethylene hydrogenation over copper-magnesia catalysts was performed. Two different approaches have been tested in order to determine which experimental data are really necessary to rapidly discriminate between different kinetic models and to reach the best precision for parameter estimation. Sequential designs allow to identify more rapidly the best kinetic model and a good parameter estimation is achieved with only a few observations. So comparing to octagonal designs, sequential designs limit experimental efforts. The best model involves a Langmuir–Hinshelwood mechanism with non-competing adsorption of hydrogen and ethylene, where the rate-determining step is either the addition of molecularly adsorbed hydrogen or the addition of the second atom of hydrogen adsorbed dissociatively. In such a case, the hydrogen adsorption should be weak enough to be neglected. Furthermore, initial reaction rates have been corrected to reach the same activity level for each measurement. The conclusion of parametric adjustment on different experimental designs is that the four octagonal designs, the two sequential designs and the two designs varying the temperature for the central point of octagonal designs are not necessary to determine parameters with a good precision. The repetition of octagonal designs is useless, and the precision obtained with octagonal or sequential designs is of the same order of magnitude. Furthermore, only the four first observations of sequential designs are enough to reach this precision. So sequential designs allow to estimate parameters more rapidly. The activation energy of the kinetic constant, the adsorption enthalpy and the adsorption entropy were found

to be equal to 63 kJ mol^{-1}, −63 kJ mol^{-1}, −133 J mol^{-1} K^{-1}, respectively, in agreement with previous studies.

Acknowledgments

Sophie L. Pirard is grateful to the National Funds for Scientific Research, Belgium (FNRS) for a Ph.D. grant. The authors also thank the Belgian Fonds pour la Recherche Fondamentale Collective (FRFC), the Région Wallonne-Direction Générale des Technologies, de la Recherche et de l'Énergie, the Ministère de la Communauté Française-Direction de la Recherche Scientifique-and the Fonds de Bay for their financial support. The involvement of the Laboratoire de Génie Chimique in the European FAME network is also acknowledged.

Appendix A

The weighted criterion proposed by Hill et al. [24] is used to optimize discrimination between models and parameter estimation. This criterion consists in balancing a discrimination criterion E and a parameter estimation criterion D.

$$C = w_1 D + w_2 E$$

where

$$D = \frac{K_\mathrm{v}}{K_{\mathrm{v,max}}}$$

$$E = \sum_{r=1}^{v} P_r^{(n)} \frac{\Delta_r}{\Delta_{r,\max}}$$

$$w_1 = \left[\frac{v(1 - P_\mathrm{b}^{(n)})}{(v-1)}\right]^{\lambda} \quad \text{with } 0 < \lambda < \infty$$

$$w_2 = 1 - w_1$$

The criterion K_v consists in researching experimental point maximizing differences between models. In the same way, optimizing Δ_r consists in researching experimental points providing the best parameter estimation for model r. $K_{\mathrm{v,max}}$ and $\Delta_{r,\max}$ are, respectively, maximal values of K_v and Δ_r in experimental area. $P_r^{(n)}$ is the probability related to model r after n observations. Subscript b corresponds to the best model, *i.e.* model for which probability $P_r^{(n)}$ is maximal. If uncertainty of each model is the same, $P_r^{(0)} = 1/v$ and consequently, $w_1 = 1$ and $w_2 = 0$. So the Hill et al. criterion is reduced to the discrimination criterion D. If $P_\mathrm{n}^{(\mathrm{b})} = 1$, $w_1 = 0$ and $w_2 = 1$. So the Hill et al. criterion is reduced to the parameter estimation criterion D. The value of λ can be fixed freely. High values support parameter estimation, while low values support model discrimination.

References

[1] I. Horiuti, M. Polanyi, Trans. Faraday Sci. 30 (1934) 1164–1172.
[2] L. Razon, R. Schmitz, Chem. Eng. Sci. 42 (1987) 1005–1012.
[3] B.E. Bent, Chem. Rev. 96 (1996) 1361–1369.
[4] F. Gao, Y. Wang, W.T. Tysoe, J. Mol. Catal. A 249 (2006) 111–122.
[5] S.D. Jackson, F.J. Robertson, J. Willis, J. Mol. Catal. 63 (1990) 255–268.
[6] H.J. Zeiger, B. Wasserman, M.S. Dresselhaus, G. Dresselhaus, Surf. Sci. 124 (1983) 583–586.
[7] M. Sprock, M. Pruski, B.C. Gerstein, T.S. King, Catal. Lett. 5 (1990) 395–402.
[8] M.M. Hills, J.E. Parmeter, W.H. Weinberg, J. Am. Chem. Soc. 108 (1986) 7215–7224.
[9] D. Stacchiola, S. Azard, L. Burkholder, W.T. Tysoe, J. Phys. Chem. 105 (2001) 11233–11240.
[10] F. Zaera, J. Phys. Chem. 94 (1990) 5090–5099.
[11] C. Egawa, S. Katamaya, S. Oki, Chem. Phys. Lett. 266 (1997) 169–172.
[12] C. Egawa, S. Katayama, S. Oki, Surf. Sci. 387 (1997) L1035–L1040.
[13] T. Sekitani, T. Teraoka, M. Fujisawa, M. Nishijima, J. Phys. Chem. 96 (1992) 8462–8471.
[14] C. Egawa, S. Osawa, S. Oki, Surf. Sci. 529 (2003) 349–358.
[15] C. Egawa, S. Oki, M. Kaneko, N. Minami, I. Suzuki, Surf. Sci. 427 (1999) 268–271.
[16] J.P. Pirard, B. Kalitventzeff, Ind. Eng. Chem. Fundam. 17 (1978) 11–18.
[17] E.G. Derouane, J.P. Pirard, G.A. L'Homme, E. Fabry, in: B. Delmon, G. Jannes (Eds.), Catalysis: Heterogeneous and Homogeneous, Elsevier, Amsterdam, The Netherlands, 1975, pp. 275–287.
[18] C. Egawa, H. Iwai, S. Oki, Surf. Sci. 454 (2000) 347–351.
[19] R.A. van Santen, J.W. Niemantsverdriet, Chemical Kinetics and Catalysis, Plenum Press, New York, 1995.
[20] J.A. Dumesic, D.F. Rudd, L.M. Aparicio, J.E. Rekoske, A.A. Treviño, The Microkinetics of Heterogeneous Catalysis, American Chemical Society, Washington, DC, 1993.
[21] G.C. Bond, Catalysis by Metals, Academic Press, New York, 1962.
[22] G. Ghiotti, F. Boccuzzi, A. Chiorino, Stud. Surf. Sci. Catal. 48 (1989) 415–423.
[23] B. Heinrichs, J.-P. Schoebrechts, J.-P. Pirard, J. Catal. 200 (2001) 309–320.
[24] W.J. Hill, W.G. Hunter, D.W. Wichern, Technometrics 10 (1968) 145–149.
[25] D.M. Himmelblau, Process Analysis by Statistical Methods, Wiley, New York, USA, 1970.
[26] Yonathan, B. Nonlinear Parameter Estimation and Programming (NLPE), I.B.M. Contributed Program Library, 360 D, 1967.
[27] F. Kapteijn, J.A. Moulijn, in: G. Ertl, H. Knözinger, J. Weitkamp (Eds.), Handbook of Heterogeneous Catalysis, vol. 3, Wiley-VCH, Weinheim, 1997, p. 1189.
[28] P.E. Gill, W. Murray, M.H. Wright, Practical Optimization, Academic Press, California, USA, 1981.
[29] D.C. Montgomery, Design and Analysis of Experiments, fifth ed., Wiley, New York, USA, 1997.
[30] M. Boudart, G. Djéga-Mariadassou, Cinétique des réactions en catalyse hétérogène, Masson, Paris, 1982.
[31] J.S. Campbell, P.H. Emmett, J. Catal. 7 (1967) 252–262.
[32] R. Hirschl, A. Eichler, J. Hafner, J. Catal. 226 (2004) 273–282.
[33] D. Duca, G. La Manna, M.R. Russo, Phys. Chem. Chem. Phys. 1 (1999) 1375–1382.
[34] E.W. Hansen, M. Neurock, J. Catal. 196 (2000) 241–252.
[35] O. Beeck, Rev. Mod. Phys. 17 (1945) 61–69.
[36] Y. Takasu, T. Sakuma, Y. Matsuda, Chem. Lett. 48 (1985) 1179–1187.
[37] R. Davis, M. Boudart, Catal. Sci. Technol. 1 (1991) 129–136.
[38] A.N.R. Bos, E.S. Bootsma, F. Foeth, H.W.J. Sleyster, K.R. Westerterp, Chem. Eng. Proc. 32 (1993) 53–61.
[39] X. Guo, R. Madix, J. Catal. 155 (1995) 336–343.
[40] T.P. Beebe, J.T. Yates, J. Am. Chem. Soc. 108 (1986) 663–672.
[41] R. Cortright, S. Goddard, J. Reskoske, J. Dumesic, J. Catal. 127 (1991) 342–351.
[42] S. Goddard, R. Cortright, J. Dumesic, J. Catal. 137 (1992) 186–193.